

Bursting behavior of the Galactic Center faint X-ray transient GRS 1741.9–2853

G. Trap^{1,2,*}, M. Falanga^{1,3}, A. Goldwurm^{1,2}, E. Bozzo^{4,5}, R. Terrier²,
P. Ferrando^{1,2}, D. Porquet⁶, N. Grosso⁶, and M. Sakano⁷

¹ Service d’Astrophysique (SAp) / IRFU / DSM / CEA Saclay – Bât. 709, 91191 Gif-sur-Yvette Cedex, France

² AstroParticule & Cosmologie (APC) / Université Paris VII / CNRS / CEA / Observatoire de Paris – Bât. Condorcet, 10, rue Alice Domon et Léonie Duquet, 75205 Paris Cedex 13, France

³ International Space Science Institute (ISSI), Hallerstrasse 6, CH-3012 Bern, Switzerland

⁴ Istituto Nazionale Di Astrofisica (INAF) / Osservatorio Astronomico di Roma, Via Frascati 33, Monte Porzio Catone, 00044 Rome, Italy

⁵ INTEGRAL Science Data Center (ISDC) / Science data center for Astrophysics, Ch. d’Ecogia 16, CH-1290 Versoix (Ge), Switzerland

⁶ Observatoire astronomique de Strasbourg / Université de Strasbourg / CNRS / INSU – 11, rue de l’Université, 67000 Strasbourg, France

⁷ Department of Physics and Astronomy / University of Leicester – LE1 7RH Leicester, UK

Received ... ; accepted ...

ABSTRACT

Aims. The neutron star low-mass X-ray binary GRS 1741.9–2853 is a known type-I burster of the Galactic Center. It is transient, faint, and located in a very crowded region, only 10' from the supermassive black hole Sgr A*. Therefore, its bursting behavior has been poorly studied so far. In particular, its persistent emission has rarely been detected between consecutive bursts, due to lack of sensitivity or confusion. This is what made GRS 1741.9–2853 one of the nine "burst-only sources" identified by *BeppoSAX* a few years ago. The physical properties of GRS 1741.9–2853 bursts are yet of great interest since we know very little about the nuclear regimes at stake in low accretion rate bursters. We examine here for the first time several bursts in relation with the persistent emission of the source, using *INTEGRAL*, *XMM-Newton*, and *Swift* observations.

Methods. We investigate the source flux variability and bursting behavior during its 2005 and 2007 long outbursts. These events were almost entirely covered by *INTEGRAL*, both in the soft (3–20 keV) and hard (20–100 keV) X-ray bands, and also partly by *XMM-Newton* and *Swift* (2–10 keV) in 2007.

Results. In its last activity periods, 2005 and 2007, the persistent luminosity of GRS 1741.9–2853 varied between ~ 1.7 and 10.5×10^{36} erg s⁻¹, i.e. 0.9 – 5.3% of the Eddington luminosity. The shape of the spectrum as described by an absorbed power-law remained with a photon index $\Gamma \approx 2$ and a column density $N_{\text{H}} \approx 12 \times 10^{22}$ cm⁻² throughout the outbursts. We discovered 11 type-I bursts with *INTEGRAL*, and inspected four additional bursts: two recorded by *XMM-Newton* and two by *Swift*. From the brightest burst, we derive an upper limit on the source distance of ~ 7 kpc. The observed bursts characteristics and source accretion rate suggest pure helium explosions igniting at column depths $y_{\text{ign}} \approx 0.8 - 4.8 \times 10^8$ g cm⁻², for typical energy releases of $\sim 1.2 - 7.4 \times 10^{39}$ erg.

Key words. Galaxy: center – Stars: neutron – X-rays: individuals: GRS 1741.9–2853 – X-rays: binaries – X-rays: bursts

1. Introduction

A low-mass X-ray binary (LMXB) is a stellar system consisting of a low mass star ($< 1 M_{\odot}$) filling its Roche lobe and pouring matter onto a compact object via an accretion disk. A large fraction ($\sim 55\%$) of the LMXB of our galaxy are transient (see Liu et al. 2007, for a recent catalogue), which means they display bright X-ray outbursts from time to time, lasting from weeks to months. During such an event, they typically increase their luminosity by a factor of at least a hundred compared to the dim state in which they spend most of their time and are usually too faint to be detected. One traditionally distinguishes three classes of transients according to their 2–10 keV peak luminosities: *bright* transients (10^{37-38} erg s⁻¹), *faint* transients (10^{36-37} erg s⁻¹), and *very faint* transients (10^{34-36} erg s⁻¹) (e.g., Wijnands et al. 2006). In particular, *faint* transients were recognized as a distinctive class with the observations of *BeppoSAX* a decade ago (Heise

et al. 1999). Just like for other transients, the outbursts of the faint ones can be accommodated by the classical disk instability model (King & Ritter 1998; Lasota 2001, for a review), provided their orbital periods are shorter than 80 min (King 2000). Yet, these faint transients are markedly concentrated towards the Galactic Center (GC) (in't Zand 2001), and generally harbor a neutron star as compact object, which is inferred from the presence of type-I X-ray bursts in the light curves of such systems. Indeed, type-I bursts are thought to result from thermonuclear explosions on the solid surface of the neutron star: see Lewin et al. (1993); Strohmayer & Bildsten (2006) for reviews, and Cornelisse et al. (2003); Galloway et al. (2008); Chelovekov et al. (2007) for recent catalogues. Interestingly, the properties of the bursts are tightly bound to the accretion rate of the neutron star. Early theoretical work by Fujimoto et al. (1981) showed that, at low accretion rates, the bursts should be triggered by the unstable burning of accreted hydrogen and should thus be dissimilar to the usual "pure helium" bursts encountered at higher

* e-mail: trap@apc.univ-paris7.fr

accretion rates. From an observational stand point, the study of low accretion rate bursters developed with the discovery of nine “burst-only sources” by *BeppoSAX* (Cocchi et al. 2001; Cornelisse et al. 2004). Indeed, the persistent emission—and so the accretion rate—of these objects was so low that the source could never be detected right before and after the bursts. This subclass of sources also recently motivated theoretical studies suggesting that, at the lowest accretion rates, unstable H burning triggers vigorous He flashes in a H-rich environment, whereas at slightly higher accretion rates, weak pure H flashes build up a thick He layer underneath the surface (Peng et al. 2007; Cooper & Narayan 2007). This layer can eventually ignite, leading to a several minutes long burst. Dim bursters could therefore possibly help bridge the gap between short bursts and the growing set of intermediate long bursts brought to light in the past 10 years (Falanga et al. 2008, 2009, and references therein). We also emphasize that almost all currently known X-ray recycled millisecond pulsars are faint LMXB transients (Wijnands 2006; Falanga 2008), making these sources interesting targets to look for fast rotators.

In this context, we present the observational analysis of one of the “burst-only sources”, GRS 1741.9–2853, with all the data pertaining to the GC ever collected by *INTEGRAL* and *XMM-Newton* since February 2002, and *Swift* data from early 2007.

1.1. History of GRS 1741.9–2853 from 1990 to 2004

GRS 1741.9–2853 was discovered in the GC in spring 1990 by ART-P, the low energy instrument onboard the *Granat* satellite (Sunyaev 1990; Sunyaev et al. 1991). The source was seen at a constant flux level of 2×10^{-10} erg s⁻¹ cm⁻² (4–30 keV) during two observations in March and April, and was also present in the mosaics of *Granat* high energy instrument SIGMA (40–100 keV, Goldwurm 1996). But in all the following campaigns on the GC however, *Granat* failed to detect GRS 1741.9–2853, establishing the source as transient. Note that this binary is only 10′ from the Milky Way supermassive black hole Sgr A*, and was thus in the field of view (FOV) of numerous observations carried out by high energy satellites over the years (see below). In September of 1994, *ASCA* identified GRS 1741.9–2853 (a.k.a. AX J1745.0–2855) back in outburst with a flux of 1.8×10^{-12} erg s⁻¹ cm⁻² in the 0.7–10 keV band (Sakano et al. 2002).

Two years later (August and September 1996), *BeppoSAX* recorded three type-I X-ray bursts from GRS 1741.9–2853 with its Wide Field Camera (Cocchi et al. 1999), implying that the source is a LMXB housing an accreting neutron star. From a photospheric radius expansion (PRE) episode in the brightest burst, Cocchi et al. (1999) derived a distance of ~8 kpc for GRS 1741.9–2853, placing it close to the very center of the galaxy. This was based on the assumption that, during PRE, the bolometric peak luminosity of a burst saturates at the Eddington luminosity and thus acts as a standard candle (Lewin et al. 1993; Kuulkers et al. 2003). Note that *BeppoSAX* could not measure the persistent flux of the source and set an upper limit on the bolometric luminosity of $\sim 1.6 \times 10^{36}$ erg s⁻¹, which made this burster another member of the “burst-only sources” class (Cornelisse et al. 2004). A little earlier in 1996, from April to July, *RXTE* scanned the GC and detected eight bright bursts from an unidentified source in this intricate region. Even though the FOV of *RXTE*/PCA contained many bursters, Galloway et al. (2008) attributed the bursts to GRS 1741.9–2853 in light of the activity seen by *BeppoSAX* at roughly the same time and the similarity between the bursts caught by the two satellites. Interestingly, three of the *RXTE* bursts showed burst oscillations

at a frequency of 589 Hz (Strohmayer et al. 1997), so that if the association of the source and the bursts holds, the neutron star in GRS 1741.9–2853 is spinning with a period of only 1.7 ms. Due to confusion, the PCA could not measure the persistent flux of the source. Unlike *RXTE*, *ASCA* managed to detect this persistent emission from GRS 1741.9–2853 in September 1996 (Sakano et al. 2002), and so strengthened the association of the *RXTE* and *BeppoSAX* bursts into a long outburst of the source that lasted at least six months. Thanks to good statistics, physical spectral parameters were constrained. The persistent emission X-ray spectrum was fitted with a photoelectrically absorbed power-law model, whose parameters are the column density, $N_{\text{H}} = 11.4_{-0.8}^{+0.9} \times 10^{22}$ cm⁻², and the spectral photon index, $\Gamma = 2.36 \pm 0.16$. The average flux was 1×10^{-10} erg s⁻¹ cm⁻² (0.7–10 keV).

The binary was undetected during another four years, until *Chandra* witnessed the source in outburst in fall 2000, with an associated weak thermonuclear burst (Muno et al. 2003)¹. These authors fitted the spectrum of the persistent emission with an absorbed power-law, $N_{\text{H}} = (9.7 \pm 0.2) \times 10^{22}$ cm⁻² and $\Gamma = 1.88 \pm 0.04$. They found the source in quiescence in summer 2001 too, at a luminosity of $\sim 10^{32}$ erg s⁻¹ (2–8 keV). These *Chandra* measurements provided the most accurate position of GRS 1741.9–2853 to date: $\alpha = 17^{\text{h}}45^{\text{m}}2.33^{\text{s}}$, $\delta = -28^{\circ}54'49.7''$ (J2000), with an uncertainty of 0.7″. By browsing the *XMM-Newton* archive, we found that in October 2002 GRS 1741.9–2853 was again weakly active at a luminosity of $\sim 10^{35}$ erg s⁻¹ (2–8 keV) (see Sect. 3.2.1.), which is somewhat reminiscent of the weak outburst captured by *ASCA* in 1994. *XMM-Newton* upper limits on the burster flux until 2004 are given in Tab. 1.

1.2. The 2005 and 2007 outbursts

From February to April 2005, the hard X-ray imager *INTEGRAL*/IBIS/ISGRI perceived a new outburst from GRS 1741.9–2853 (Kuulkers et al. 2007c). The source was temporarily called IGR J17453–2853 until it was later recognized as GRS 1741.9–2853 (Kuulkers et al. 2007b). *Chandra* found the source still in activity in June (Wijnands et al. 2005) and slowly fading one month later (Wijnands et al. 2006). The July spectrum of the source was similar to the previous *Chandra* fit published earlier by Muno et al. (2003): $N_{\text{H}} = 10.5_{-3.7}^{+4.9} \times 10^{22}$ cm⁻² and $\Gamma = 1.8_{-0.8}^{+1.0}$. These observations triggered an optical follow-up in the I band, that could not identify any visible counterpart (Laycock et al. 2005), in accordance with the high reddening expected from GC sources. As we will explain below (Section 3.1.2), during this at least 3 months long outburst, we found 4 type-I X-ray bursts with *INTEGRAL*/JEM-X.

In 2007, renewed activity from GRS 1741.9–2853 was detected by several observatories. In February, *INTEGRAL* started a new long exposure on the Galactic Bulge, and clearly caught the source in activity (Kuulkers et al. 2007a,b). The satellite monitored the outburst all the way to April when the source went back to quiescence. We discovered a total of seven bursts distributed between March and April (see Sect. 3.1.2). The early detection of the source by *INTEGRAL* triggered a short pointing with *Swift*/XRT which detected a new X-ray burst (Wijnands et al. 2007). It is likely that another burst of GRS 1741.9–2853 was also detected by *Swift*/BAT earlier, in January (Fox et al. 2007). These two bursts are also inspected in Section 3.3.2 of the present paper. From March to April, *Swift*/XRT followed

¹ GRS 1741.9–2853 is also known as CXOGC J174502.3–285450 in the *Chandra* catalogue (Muno et al. 2006).

Table 1. GRS 1741.9–2853 flux history.

Date	Instrument	Flux ^a [10 ⁻¹¹ erg s ⁻¹ cm ⁻²]	Ref. ^b
1990–2002	[1]
2002 Feb 26	<i>XMM-Newton</i> /PN	< 0.0007	[2]
2002 Oct 3	<i>XMM-Newton</i> /PN	1	[2]
2004 Mar 28	<i>XMM-Newton</i> /PN	< 0.0007	[2]
2004 Aug 31	<i>XMM-Newton</i> /PN	< 0.0002	[2]
2005 Apr 10	<i>INTEGRAL</i> /ISGRI	31.9	[3],[4]
2005 Jun 5	<i>Chandra</i> /HRC	10	[5],[6]
2005 Jul 1	<i>Chandra</i> /ACIS	1.7	[5],[6]
2006 Feb 27	<i>XMM-Newton</i> /PN	< 0.0058	[2]
2006 Sep 8	<i>XMM-Newton</i> /PN	< 0.0057	[2]
2006 Sep ~20	<i>Swift</i> /XRT	1.2	[7]
2007 Feb 15	<i>INTEGRAL</i> /ISGRI	13	[4],[8]
2007 Feb 16	<i>Swift</i> /XRT	15	[9],[2]
2007 Feb 22	<i>Chandra</i> /ACIS	3	[10]
2007 Feb 27	<i>XMM-Newton</i> /PN	11.6	[2]
2007 Mar	<i>Swift</i> /XRT	26	[7]
2007 Apr 2	<i>XMM-Newton</i> /PN	13.1	[11],[2]
2007 Apr 4	<i>XMM-Newton</i> /PN	5.5	[11],[2]
2007 Sep 6	<i>XMM-Newton</i> /PN	< 0.0026	[2]
2008 Mar 23	<i>XMM-Newton</i> /PN	< 0.0003	[2]

^a X-ray flux in the ranges 2–8 keV for *XMM-Newton* and *Chandra*, 20–60 keV for *INTEGRAL*/ISGRI, 3–10 keV for *INTEGRAL*/JEM-X, and 2–10 keV for *Swift*/XRT.

^b References: [1] Muno et al. (2003), [2] This work, [3] Kuulkers et al. (2007c), [4] Kuulkers et al. (2007b), [5] Wijnands et al. (2005), [6] Wijnands et al. (2006), [7] Degenaar & Wijnands (2009), [8] Kuulkers et al. (2007a), [9] Wijnands et al. (2007), [10] Muno et al. (2007), [11] Porquet et al. (2007).

the source more regularly, and measured the peak of the outburst at a luminosity of $\sim 2 \times 10^{36}$ erg s⁻¹ (2–10 keV) (Degenaar & Wijnands 2009). The latter authors fitted the average spectrum with $N_{\text{H}} = 14_{-0.9}^{+1} \times 10^{22}$ cm⁻² and $\Gamma = 2.6 \pm 0.2$. They also noticed the presence of a short (one week long) and faint ($\sim 10^{35}$ erg s⁻¹) outburst of the source in September 2006, that might have been a precursor to the 2007 longer outburst. *Chandra* measured the persistent luminosity of GRS 1741.9–2853 on February 22nd: 4×10^{35} erg s⁻¹ ($N_{\text{H}} = 9 \pm 0.5 \times 10^{22}$ cm⁻² and $\Gamma = 0.9 \pm 0.1$, 2–8 keV) (Muno et al. 2007). On February 27th, an *XMM-Newton*/PN observation was carried out in Timing mode to search for millisecond pulsations in the persistent emission and burst oscillations. Yet, neither was a burst recorded nor was any pulsation found (Wijnands 2008). Finally, *XMM-Newton* was pointed once again to the GC at the beginning of April as part of a multiwavelength campaign on the supermassive black hole Sgr A* (Porquet et al. 2008; Trap et al. 2009; Dodds-Eden et al. 2009). This long observation (~ 100 ks) coincided with the end of GRS 1741.9–2853 outburst and contains two type-I bursts (Porquet et al. 2007); we examine these in greater details in Section 3.2.2.

To sum up GRS 1741.9–2853 flux history, we have updated in Fig. 1 the long term light curves extracted from Muno et al. (2003) and Wijnands et al. (2006), with data spanning from 2002 to 2007 (Table 1). Over the past 18 years, the X-ray luminosity of GRS 1741.9–2853 varied regularly from 10^{32} erg s⁻¹ in quiescence, up to 10^{36} erg s⁻¹ in outburst, justifying the source classification of faint soft X-ray transient.

2. Observations and data analysis

2.1. INTEGRAL

The *INTEGRAL* satellite (Winkler et al. 2003) has been regularly scanning the GC twice a year, in spring and fall, since the beginning of the mission in October 2002. Hereafter, we take into account the data of the Joint European X-ray Monitor (JEM-X), module 1 and 2 (Lund et al. 2003), between 3 and 20 keV, and the *INTEGRAL* Soft Gamma-Ray Imager (ISGRI, 20–100 keV) (Lebrun et al. 2003), from the Imager on Board the *INTEGRAL* Satellite (IBIS) (Ubertini et al. 2003). The data were processed with the standard Offline Science Analysis (OSA) software package, version 7.0, distributed by the *INTEGRAL* Science Data Center (Courvoisier et al. 2003) and based on algorithms described in Goldwurm et al. (2003) for IBIS, and Westergaard et al. (2003) for JEM-X.

To search for periods of activity of GRS 1741.9–2853 with JEM-X, we selected all the public data since the launch of the satellite, pointing less than 3.5° away from the source position. The available data consist of 2626 usable individual pointings. These single pointings were first deconvolved and analyzed separately. We then divided this dataset into six months periods and combined the corresponding individual pointings into mosaics. GRS 1741.9–2853 was clearly detected only during two periods, from February to April 2005 and February to April 2007, at a significance level of 21σ and 12σ , respectively. Figure 2 (upper panel) shows the significance map of the GC region, in the 3–20 keV energy range, for the 2007 dataset. Many sources are present in the FOV of all the mosaics, but thanks to JEM-X high angular resolution (3.3' FWHM at best, Brandt et al. 2003), GRS 1741.9–2853 is free of contamination from the neighboring objects. Thereafter, we concentrate on these two epochs, 2005 and 2007, which gather 417 and 253 individual pointings of ~ 1.8 ks each, for total effective exposures of about 397 ks and 242 ks, respectively.

2.2. XMM-Newton

GRS 1741.9–2853 has been detected on three occasions by the *XMM-Newton* satellite (Jansen et al. 2001) operating in different instrument configurations (see Table 2 for a journal of the observations): October 2002, February 2007, and March/April 2007. The Science Analysis Software (SAS, version 7.1.2) and the latest Current Calibration files (CCFs) were used to produce calibrated event lists from the Observation Data Files (ODFs). PN event lists were then filtered with the standard selection criteria `Flag=0` in order to remove bad pixels, hot pixels, and pixels close to CCD gaps.

For all the observations, we computed the light curve of the whole detector in the 10–12 keV energy range to identify the time intervals contaminated by background soft proton flares. We excluded from our analysis all the phases where this background count rate exceeded 100 counts per time bins of 100 s. In particular, the last seven hours of both rev-1339 and rev-1340 were rejected in this context. Apart from rev-1322, where the standard technique for Timing data was applied, all spectra from the persistent emission were extracted from a circular region of 50' radius, encircling 90% of the Point Spread Function (PSF) of the instrument. Background counts were obtained from a similar region offset from the source position. Because the bursts periods were affected by pile-up, special care was taken for the light curves and spectra of these time intervals: events from the inner 6'' of the PSF were ignored and the parameter `Pat` tern was

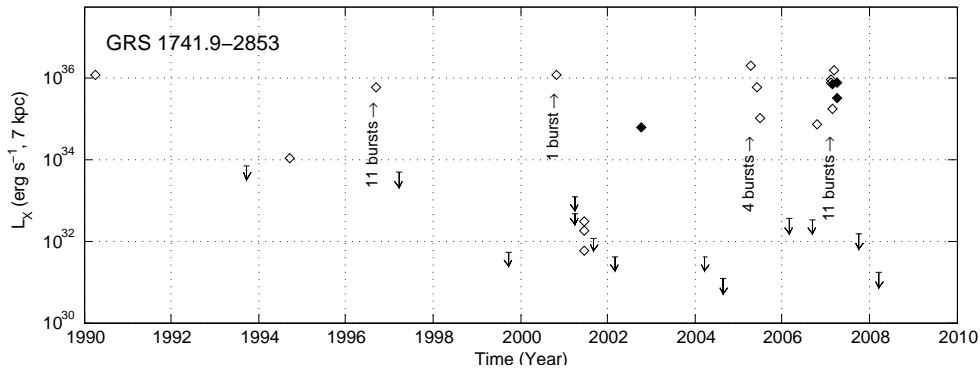


Fig. 1. X-ray luminosity history of GRS 1741.9–2853. Open diamonds and upper limits before 2002 correspond to data published elsewhere, and filled diamonds to the *XMM-Newton* measurements reported here. See Table 1 for the respective energy ranges of the different points. We indicate the total number of bursts detected during each outburst by *BeppoSAX*, *RXTE*, *Chandra*, *INTEGRAL*, *Swift*, and *XMM-Newton*.

Table 2. *XMM-Newton*/PN and *Swift*/XRT log of the observations used in this paper.

Orbit	ObsID	Date Start [UTC]	Exposure [ks]	Mode ^a
<i>XMM-Newton</i> /PN				
406	111350101	2002 Feb 26, 06:41:42	40.0	Imaging (T)
516	111350301	2002 Oct 3, 07: 17:07	15.3	Imaging (T)
788	202670501	2004 Mar 28, 16:45:33	41.9	Imaging (M)
866	202670701	2004 Aug 31, 03:34:59	126.7	Imaging (M)
1139	302882601	2006 Feb 27, 04:27:37	0.5	Imaging (M)
1236	302884001	2006 Sep 8, 17:19:46	0.5	Imaging (M)
1322	506291201	2007 Feb 27, 06:27:39	37.6	Timing (M)
1338	402430701	2007 Mar 30, 21:28:14	32.3	Imaging (M)
1339	402430301	2007 Apr 1, 15:07:59	103.5	Imaging (M)
1340	402430401	2007 Apr 3, 16:39:17	97.6	Imaging (M)
1418	504940201	2007 Sep 6, 10:28:34	11.1	Imaging (M)
1518	505670101	2008 Mar 23, 17:22:10	96.6	Imaging (M)
<i>Swift</i> /XRT				
...	0003088801	2007 Feb 16, 21:39:18	3.9	Photon counting

^a The *XMM-Newton* optical filter employed is given in brackets: T and M stand for Thick and Medium, respectively.

set to zero to reject all but single events. For each burst, we took the persistent emission before the burst as background. Version 11.3.2. of the XSPEC software (Arnaud 1996) was used to fit all the spectra with physical models. Errors are quoted at 90% confidence level for one parameter of interest.

Concerning the observations where GRS 1741.9–2853 was not active, i.e. February 2002, March/August 2004, February/September 2006, September 2007, and March 2008, we calculated 3σ upper limits in counts s^{-1} with *ximage* and converted them into 2–8 keV unabsorbed fluxes thanks to *WebPIMMS*. Results are summarized in Table 1.

2.3. *Swift*

For the present study we used the publicly accessible observations id. 00257213000 and 00030888001 from *Swift* (Gehrels et al. 2004). The first dataset includes the burst discovered on January 22nd, 2007 with the high energy coded mask detector BAT (Fox et al. 2007), whereas the second comprises both the burst and the persistent emission observed with the low energy telescope XRT on February 16–17th, 2007 (Wijnands et al. 2007). After the burst detected by the *Swift*/BAT on January

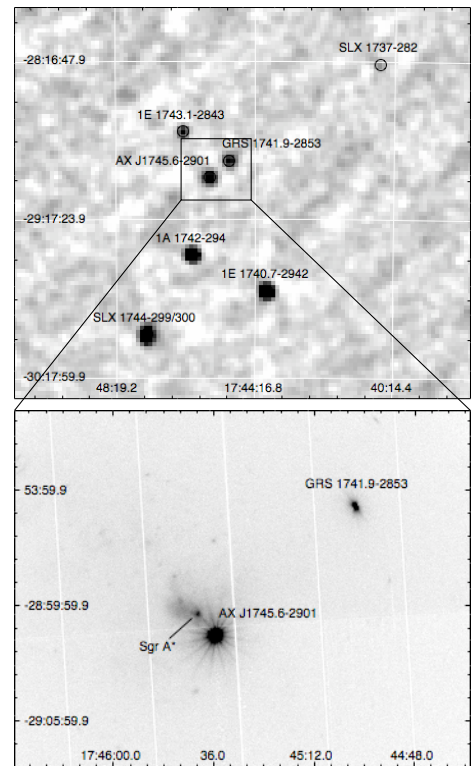


Fig. 2. *INTEGRAL*/JEM-X 3–20 keV significance mosaic (top panel) constructed from 253 individual pointings between February and April 2007, with an effective exposure of 242 ks at the position of GRS 1741.9–2853. Equatorial coordinates are used and the galactic plane runs from upper left to bottom right. The magnified view (lower panel) is an *XMM-Newton*/PN 0.1–10 keV image in April 2007 (rev-1340, 97.6 ks exposure). Sgr A*, the supermassive black hole of the Galactic Center, is clearly apparent since this observation contains several flares from the vicinity of the black hole, enhancing its average luminosity (Porquet et al. 2008).

22nd, no XRT follow-up has been performed. The total exposure time was ~ 4 ks for BAT during observation 00257213000, and ~ 3.9 ks for XRT during observation 00030888001.

For the BAT data analysis, we used the `batgrbproduct` tool included in the `Heasoft` package 6.6.1. The BAT spectrum has been extracted over the entire duration of the burst (9 s). The XRT data were processed with the `xrtpipeline` (version 0.12.1) task. Filtering and screening criteria were applied by using the `ftools` (`Heasoft` version 6.6.1). We analyzed data in photon counting (PC) mode, and selected event grades of 0–12. All the XRT/PC data were affected by a strong pile-up, and thus we extracted the source light curves and spectra by using annular regions centered on the source. The persistent light curves and spectra were extracted through an annular region with an inner radius of 4 pixels and an external radius of 20 pixels. Unfortunately, the count rate during the burst was very high and the corresponding pile-up was much stronger than that of the persistent emission. In order to correct for this effect, we used annular regions with different inner radii during the rise, the peak and the decay of the burst (the inner radii were of 10, 15 and 4 pixels, respectively). We then used the `xrt1ccorr` task to account for these corrections in the background-subtracted light curves. To estimate the spectral properties of the source and its flux during the entire burst, we used an extraction region with an inner radius of 10 pixels. All the spectra were rebinned in order to have at least 20 photons per bin so as to permit χ^2 fitting. Exposure maps were created through the `xrtexpomap` routine, and we used the latest spectral redistribution matrices in the HEASARC calibration database (version 0.1.1). Ancillary response files, accounting for different extraction regions, vignetting and PSF corrections, were generated via the `xrtmkarf` task.

3. Results

3.1. INTEGRAL

3.1.1. Outbursts

Albeit significant in the global mosaics of the 2005 and 2007 outbursts, the source was so weak that it was never significantly detected in neither JEM-X nor ISGRI individual pointings. Hence, the standard technique to derive light curves with OSA was not adequate. So, we built the light curves from the individual images, by collecting the count rate in the pixel consistent with the source position for ISGRI, and by integrating the flux over a $4.2'$ (FWHM) PSF for JEM-X². Then, by rebinning with long intervals (\sim days), the evolution of the outbursts becomes visible (see Fig. 3). In 2005, *INTEGRAL* observations ceased in April, but *Chandra* still detected the source fading in June and July (Wijnands et al. 2005, 2006) so *INTEGRAL* missed the end of the outburst. In 2007, instead, we missed the beginning and got the end. Notice that the drop in the light curve around MJD 54155 (end of April 2007) was confirmed by independent flux measurements of *Swift*, *Chandra* and *XMM-Newton* at lower energies, in the ~ 2 –10 keV band (see Table 1).

3.1.2. Type-I bursts

To search for type-I bursts, we investigated all the JEM-X, module 1 and 2, data publicly available since the beginning of the mission, pointing less than 3.5° away from the source position, and forced the standard pipeline to construct 2 s rebinned light curves. Since the persistent emission of GRS 1741.9–2853 was never detected in single pointings, these light curves contain mainly background emission and “spikes”. Most of these spikes

² The size of the PSF was empirically derived from a bright source of the FOV, GX 3+1, in the 3–20 keV range.

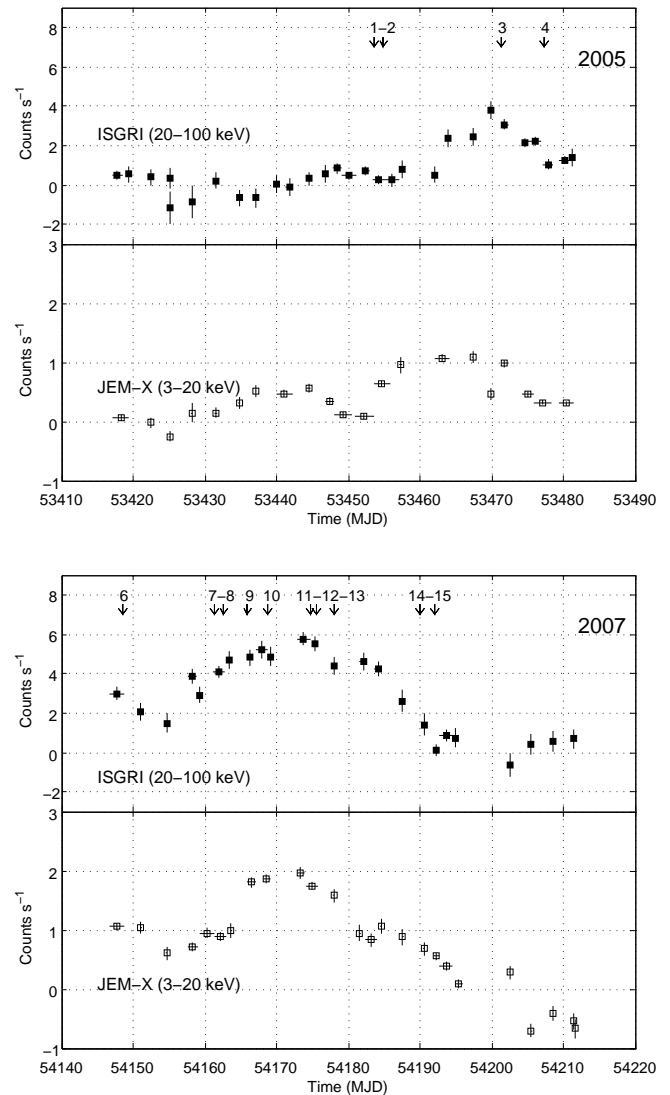


Fig. 3. *INTEGRAL*/ISGRI and JEM-X light curves of the 2005 (upper panel) and 2007 (lower panel) outbursts in the 20–100 keV and 3–20 keV bands, respectively. All the type-I bursts reported in this work are indicated by the arrows, leaving out the *Swift*/BAT burst #5 that occurred on \sim MJD 54122. Note that the error bars on the count rate and the binning times are sometime within the square symbols. Negative count rates are due to statistical fluctuations at low flux level after background subtraction.

are due to instrumental artefacts and some to contamination by bright type-I bursts from other sources in the FOV. To identify the bursts origins, we systematically built images of the sky between the beginning and the end of the bursts candidates. When a thermonuclear burst from GRS 1741.9–2853 occurs, one should locate a significant excess at the position of the source in the image. By this means, we found a total of four and seven type-I bursts from GRS 1741.9–2853 in the 2005 and 2007 outbursts, respectively, and none during the quiescent state of the source.

We looked for the high energy (18–40 keV) tails of these 11 bursts in the ISGRI data as well. Therefore, we extracted the off-axis corrected light curves with events selected according to the detector illumination pattern, using a pixel illumination fraction threshold of 0.4. Only the brightest burst, #4, could be convincingly detected in the light curve and image. In so far as the FOV

from IBIS is larger than the one of JEM-X, the total IBIS exposure on GRS 1741.9–2853 is longer and so it was worth searching for additional bursts in the IBIS data stream. To do that, we used the *INTEGRAL* Burst Alert System (IBAS) software running at ISDC and dedicated to the real time localization and discovery of gamma-ray bursts, transient X-ray sources and bursts in the IBIS/ISGRI data (Mereghetti et al. 2003). IBAS found only burst #4.

In Table 4, we report the bursts start times measured by JEM-X. The start time of each burst is defined as the time when the intensity rose to 10% of the peak above the persistent intensity level. On Figure 4, we plot the background subtracted light curves of the 11 bursts with a 2 s time bin. The background subtraction consisted in removing the constant level present before and after the bursts in the light curve of the individual pointing of interest. Note that this background was not due to the persistent emission of the source, because it was too weak to be detected in such a short period (~ 1.8 s). The rise time is the interval between the start of the burst and the time at which the intensity reaches 90% of the peak intensity. For all the bursts it was ~ 2 –4 s, except maybe for burst 4 which had an unusual morphology. The e-folding decay times, determined over the time after the peaks and plateaus, are specified in Table 4. They roughly range between 10 and 20 s. The total durations, i.e. from the burst start time back to the persistent flux level in the 3–20 keV band, were around 20–30 s.

For the spectral analysis, we used JEM-X counts during 5 s at the peak of the bursts, in the 3–20 keV band. The net peak burst spectra are well fitted by a photoelectrically absorbed black-body model (BB). Unfortunately the energy range covered by JEM-X does not allow us to constrain the interstellar hydrogen column density, N_{H} . We therefore fixed N_{H} to $12 \times 10^{22} \text{ cm}^{-2}$, the value found with *XMM-Newton* (see Sect. 3.2.1.), in all our spectral fits. The inferred BB temperatures, kT_{peak} , and apparent BB radii, R_{peak} , at 7 kpc (see section 4) are listed in Table 4, along with other bursts parameters. The peak fluxes, F_{peak} , were derived from the 3–20 keV light curves peak count rates with 2 s time resolution and renormalized for the 0.1–100 keV bolometric energy range. The bursts fluences are obtained from the fluxes extrapolated in the bolometric energy band over the respective bursts durations.

To investigate the bursting behavior of a LMXB, it is important to know its accretion rate before the bursts (see section 4). A common estimator of this parameter is the persistent luminosity of the source. Here, to assess the persistent flux before one burst, we first built JEM-X mosaics made of between 10 and 30 consecutive pointings preceding the burst in a single band (3–20 keV). Except for bursts 1 and 2 where only upper limits could be set, the persistent emission of the source was always significantly detected in the mosaics. We then converted the count rate fitted in the mosaics into a bolometric flux³, assuming one constant spectral shape throughout the outbursts, composed of an intrinsic power-law of index $\Gamma = 2$ between 0.1 and 100 keV (see Sect. 3.2.1.).

3.2. XMM-Newton

3.2.1. Persistent emission

The EPIC/PN spectra of GRS 1741.9–2853 persistent emission in 2002 and 2007 were best fitted by an absorbed power-law.

³ This count rate was compatible with the rebinned light curves on Fig. 3 but more precise.

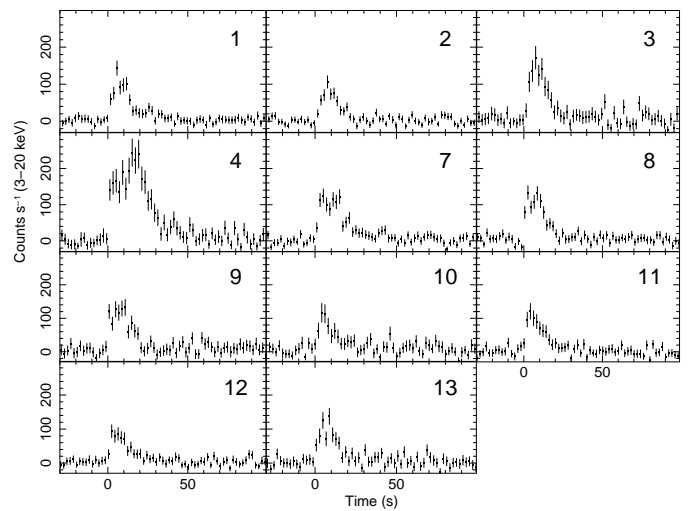


Fig. 4. Background subtracted light curves of all the bursts detected by *INTEGRAL*/JEM-X in the 3–20 keV energy range. The time bin is 2 s and the start times of the bursts are given in Table 4.

Table 3. *XMM-Newton*/PN and *Swift*/XRT spectral results for the persistent emission.

Date ^a	N_{H}^b [10^{22} cm^{-2}]	Γ	F_{pers}^c	$\chi^2/\text{d.o.f.}$
<i>XMM-Newton</i> /PN				
2002 Oct 3	14 ± 3 [11.9]	2.0 ± 0.5 1.6 ± 0.2	1.0 ± 0.2 0.9 ± 0.2	67/64 68/65
2007 Feb 27	11.9 ± 0.2	1.83 ± 0.03	11.60 ± 0.05	219/197
2007 Mar 30	11.6 ± 0.4 [11.9]	1.76 ± 0.08 1.81 ± 0.04	11.9 ± 0.1 12.2 ± 0.1	155/200 156/201
2007 Mar 31	12.1 ± 0.4 [11.9]	1.86 ± 0.08 1.83 ± 0.04	12.0 ± 0.1 11.9 ± 0.1	192/210 192/211
2007 Apr 1	12.0 ± 0.3 [11.9]	2.08 ± 0.05 2.06 ± 0.02	13.6 ± 0.1 13.5 ± 0.1	242/213 242/214
2007 Apr 2	12.5 ± 0.3 [11.9]	2.14 ± 0.05 2.04 ± 0.02	13.1 ± 0.1 12.4 ± 0.1	213/195 225/196
2007 Apr 3–4	13.1 ± 0.4 [11.9]	2.30 ± 0.08 2.08 ± 0.03	5.5 ± 0.1 4.9 ± 0.1	179/200 204/201
<i>Swift</i> /XRT				
2007 Feb 16–17	10.9 ± 3.6	1.9 ± 0.7	19.0 ± 3.0	31/28

^a For 2007, Mar 30 and 31 designate the periods just before and after burst 12 respectively (see Fig. 5). Same thing for Apr 1 and 2 and burst 13. Apr 3–4 period is the last *XMM-Newton* revolution (rev-1340).

^b Whenever there are brackets, the column density is frozen.

^c Unabsorbed flux in the 2–8 keV and 2–10 keV band in units of $10^{-11} \text{ erg s}^{-1} \text{ cm}^{-2}$ for *XMM-Newton*/PN and *Swift*/XRT, respectively.

They were fitted between 2–8 keV since, outside these bounds, there were systematic residuals due to the background. Table 3 presents the results of the best fits. We studied all the spectra with N_{H} as a free parameter. Given that we do not notice any apparent variation of N_{H} , it is most likely mainly due the galactic absorption. So, we refitted all the data consistently with N_{H} fixed to $11.9 \times 10^{22} \text{ cm}^{-2}$, the value with the smallest error found with the February 2007 pointing. In 2007, the index remained always close to 2, thus justifying the assumption we made in Sect. 3.1.2. for the persistent emission measured by JEM-X. The flux was divided by two during last orbit. For this observation, we created an image cleaned for out of time events (OoT) in the 0.1–10 keV, displayed on Fig. 2. The light curve of the three last observations in March/April 2007 are plotted in Figure 5.

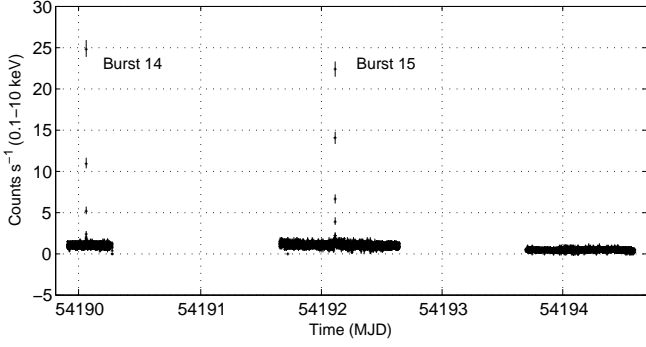


Fig. 5. *XMM-Newton*/PN background subtracted light curve of GRS 1741.9–2853 in spring 2007 (rev-1338, 1339, and 1340). Two type-I bursts, 14 and 15, are clearly visible.

3.2.2. Type-I bursts

In the light curve of the three last revolutions (Fig. 5), we clearly recognize a couple of type-I X-ray bursts (14 and 15) separated by ~ 178 ks. In view of the huge data gap between them, we cannot claim the bursts were consecutive for sure. A closer view of their net light curves (from which the persistent emission was subtracted) with a time bin of 2 s is visible on Fig. 6 (top panels). Both bursts have quick rises (~ 2 s) followed by exponential decays of about 20 s (see Table 4).

The statistics obtained with *XMM-Newton* allowed us to perform time-resolved spectral analysis of the bursts. Again, the spectra were well fitted by absorbed black-bodies with N_H fixed to $12 \times 10^{22} \text{ cm}^{-2}$. Figure 6 shows the evolution of the bolometric flux (0.1–100 keV), F_{bol} , black-body temperature, kT_{bb} , and black-body radius, R_{bb} , as a function of time. In Table 4, we report these latter values measured at the peak, as well as the fluence, f_b , integrated over the total duration of the bursts. The first event, #14, was not contemporaneous with the *INTEGRAL* GC survey, whereas #15 fell in an *INTEGRAL* observing window. Nonetheless we did not detect it neither with ISGRI nor JEM-X. The ISGRI non detection is consistent with the fact that the burst was faint, while for JEM-X the absence of detection is surely due to the position of the source in the noisy edge of the FOV.

Regarding for the persistent flux prior to the bursts, we extrapolated the results indicated in Table 3 over the 0.1–100 keV energy band.

3.3. *Swift*

3.3.1. Persistent emission

The *Swift*/XRT persistent emission spectrum of February 16–17th 2007 was fitted by an absorbed power-law model, as used for the *XMM-Newton* spectra. The best fit parameters are $N_H = 10.9 \pm 3.6 \times 10^{22} \text{ cm}^{-2}$ with a power-law photon index of $\Gamma = 1.9 \pm 0.7$ with a $\chi^2_{\text{red}} = 31.5/28$. The averaged absorbed and unabsorbed 2–10 keV fluxes were $9.8 \pm 2.5 \times 10^{-11} \text{ erg s}^{-1} \text{ cm}^{-2}$ and $19.0 \pm 0.7 \times 10^{-11} \text{ erg s}^{-1} \text{ cm}^{-2}$, respectively. These spectral parameters are in accordance with the previously reported values (Wijnands et al. 2007). Note that this observation was contemporaneous with the beginning of the *INTEGRAL*/JEM-X/ISGRI 2007 observations. The XRT unabsorbed bolometric flux 0.1–100 keV, $\sim 8.1 \times 10^{-10} \text{ erg s}^{-1} \text{ cm}^{-2}$, is comparable with the first pre-burst JEM-X flux reported in Table 4 for burst 7, which occurred at the same flux level (see light curve on Fig. 3 bottom

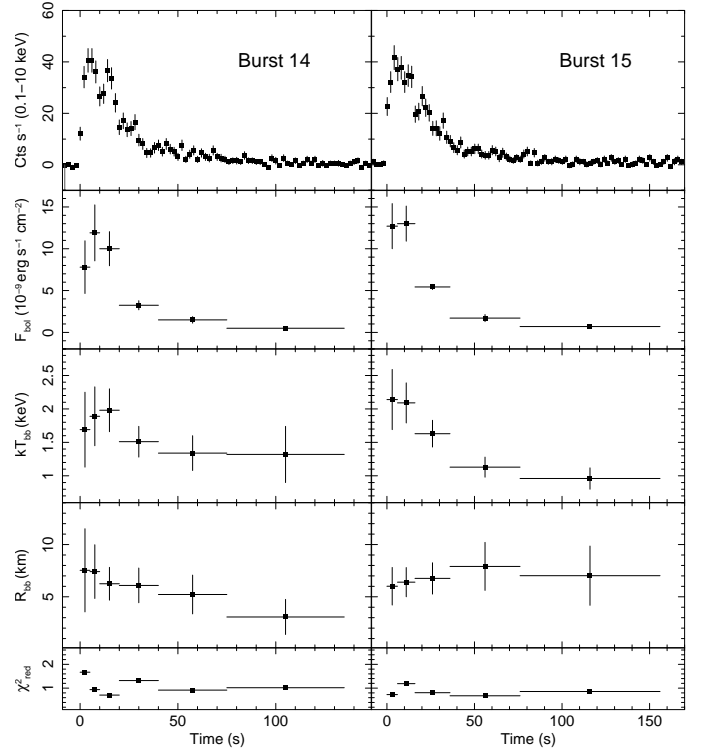


Fig. 6. Light curves and spectral evolution of bursts 14 and 15 as measured by *XMM-Newton*/PN in spring 2007. From top to bottom: count rate with a time bin of 2 s, bolometric flux estimated over 0.1–100 keV, temperature and radius of the photosphere obtained by fitting the spectra with the BB model, and reduced chi-squared of the fits.

panels). For a long term XRT light curve of GRS 1741.9–2853, we refer the reader to Fig. 2 in Degenaar & Wijnands (2009).

3.3.2. Type-I bursts

Swift detected two type-I bursts: one, #5, with BAT (15–25 keV) on January 22nd, 2007 at 06:12:54 (UTC) and another one, #6, with XRT 25.69976 days later. For the BAT burst, we cannot determine the cooling time, τ , since only the hard tail of the burst was observed. However, the rise time was around 2 s and the total burst elapsed time was 8.2 s. Due to the short exposure time, the persistent emission could not be measured, in addition, no low energy *Swift*/XRT follow-up was performed to investigate the persistent emission. The BAT and XRT light curve properties are reported in Table 4. Notice that the other burst also found at high energy was burst number 4 with *INTEGRAL*/ISGRI. In Fig. 7 we show the *Swift*/BAT and *Swift*/XRT bursts and, for comparison with BAT, the 15–25 keV ISGRI burst.

The BAT burst was not covered by the *INTEGRAL* scan of the GC and the XRT burst unluckily occurred during a slew of *INTEGRAL*, preventing the use of the data.

The spectral analysis of burst #5 was carried out in the 15–25 keV. The spectrum was well fitted by an absorbed black-body model with the column density again frozen to $12 \times 10^{22} \text{ cm}^{-2}$. The inferred bursts parameters are reported in Table 4. The measured unabsorbed flux was extrapolated to the 0.1–100 keV band by generating dummy responses with XSPEC. such an extrapolation was well justified for the JEM-X data since the black-body temperature was well inside the instrument bandpass (Sec.

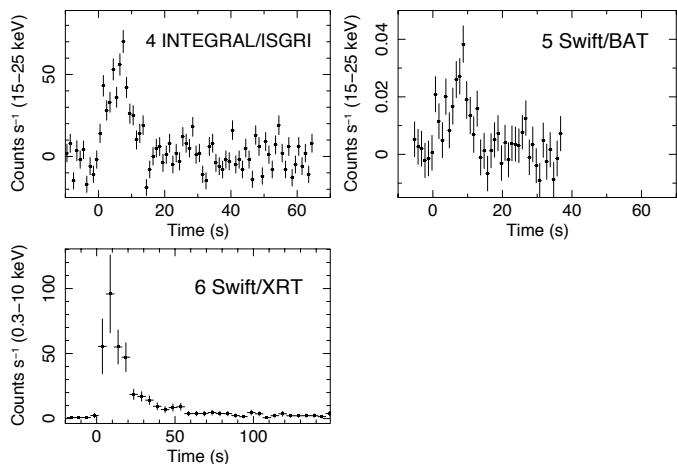


Fig. 7. Background subtracted light curves of the *Swift* bursts and the ISGRI one for comparison with the BAT one. The time bins are 1 s for #4 and #5, and 5 s for #6. The start times are given in Table 4.

3.1.2). However, this is not the case for the BAT burst, so one may question the value of $kT_{\text{bb}} = 2.4^{+0.8}_{-0.5}$ keV that we obtain by a simple extrapolation. To estimate the uncertainty introduced by this method, we focused on burst #4 and compared the fit of the ISGRI data alone and the joint JEM-X/ISGRI spectrum (3–35 keV). We find that fitting solely the high energy spectrum and extrapolating it to softer energies, leads to an error of 30%, which is inside our BAT error box and so is an acceptable method.

Due to the high count rate at the peak of burst #6, the XRT/PC image was affected by strong pile-up and a spectral analysis of the burst peak was impossible. Therefore, in order to estimate the burst peak flux, we used the parameters determined for the burst mean spectrum (N_{H} fixed at 12×10^{22} cm $^{-2}$, and BB temperature $1.6^{+0.4}_{-0.3}$ keV) and calculated the flux at the peak by using the burst peak count rate (96 ± 30 counts s $^{-1}$) and the on-line tool *webpimms*. We found an unabsorbed 0.1–100 keV flux of $2.7 \pm 0.8 \times 10^{-8}$ erg s $^{-1}$ cm $^{-2}$. The burst peak BB temperature could however be higher than the used 1.6 keV. Therefore, using *webpimms* we also estimated the peak flux for a BB temperature of 3 keV. Since this is believed to be an upper limit to the X-ray temperature at the burst peak, the corresponding X-ray flux we derived (6×10^{-8} erg s $^{-1}$ cm $^{-2}$) could be reasonably considered an upper limit on the peak X-ray flux as well.

4. Discussion

Herein, we report the monitoring by *INTEGRAL* and *XMM-Newton* of the Galactic Center faint transient GRS 1741.9–2853 in outburst during two visibility periods, 2005 and 2007. During these outbursts, the bolometric persistent flux of the source was observed to vary between ~ 0.3 and 1.8×10^{-9} erg s $^{-1}$ cm $^{-2}$, with a spectral photon index always close to 2 (Table 4 and 3). We discovered 11 type-I bursts with *INTEGRAL* and also examined four other ones: two via *XMM-Newton* and two via *Swift*, to be as complete as possible. The parameters of the eight *RXTE* bursts recently reported by Galloway et al. (2008) are very similar, i.e. peak fluxes, bursts fluences, rise times, and shapes, to those summarized in Table 4. This argues in favor of the association proposed by these authors between the bursts and the source.

The distance to the source can be determined through bursts undergoing PRE. We cannot claim any of the burst detected from GRS 1741.9–2853 reached a PRE, but from the brightest one, #4, we can calculate an upper limit on the source distance. Supposing an isotropic emission and a bolometric peak luminosity equal to the Eddington value for a pure He type-I burst (hydrogen mass fraction $X = 0$), $L_{\text{Edd}} = 3.8 \times 10^{38}$ erg s $^{-1}$, as empirically derived by Kuulkers et al. (2003), we obtain a distance upper limit $d = 7.6^{+2.0}_{-0.5}$ kpc. For comparison, the theoretical value (Lewin et al. 1993) for the upper limit found by considering a He atmosphere and a canonical neutron star ($1.4M_{\odot}$ for 10 km radius), is $6.7^{+1.8}_{-0.4}$ kpc. Note also that taking a hydrogen rich mixed burst (solar composition $X = 0.7$) would lead to a closer distance upper limit of $5.1^{+1.4}_{-0.3}$ kpc. These results are in agreement with the distance estimates made by Cocchi et al. (1999) and Galloway et al. (2008) and the measured high column density $\sim 12 \times 10^{22}$ cm $^{-2}$.

Let us assume in the following that the bursts we observed were pure He bursts ($X = 0$) and the source distance has a fiducial value $d = 7$ kpc. Then the unabsorbed bolometric persistent flux range of the source translates to luminosities $L_{\text{pers}} \approx 1.7 - 10.5 \times 10^{36}$ erg s $^{-1}$. This persistent luminosity depends upon the local accretion rate per unit area, \dot{m} , via the equation $L_{\text{pers}} = 4\pi R^2 \dot{m} (GM/R)(1+z)^{-1}$, where M and R stand for the mass and radius of the neutron star respectively, and $z = (1 - 2GM/(Rc^2))^{-1/2} - 1$ is the gravitational redshift at its surface. We consider here the canonical values $M = 1.4M_{\odot}$, $R = 10$ km, and consequently $z = 0.31$. As a result $\dot{m} \approx 1000 - 6100$ g s $^{-1}$ cm $^{-2}$. A common unit for expressing \dot{m} is the corresponding Eddington rate $\dot{m}_{\text{Edd}} = 2m_{\text{p}}c(R\sigma_{\text{Th}})^{-1}(1+X_0)^{-1}(1+z)$, where m_{p} , X_0 , c , and σ_{Th} are the proton mass, the H abundance of the matter accreted from the donor star, the speed of light, and the Thompson scattering cross section, respectively. From now on we will presume $X_0 = 0.7$ and so $\dot{m}_{\text{Edd}} = 11.5 \times 10^4$ g s $^{-1}$ cm $^{-2}$, leading to $\dot{m} \approx 0.9 - 5.3\%$ \dot{m}_{Edd} .

On the other hand, the observed fluences, f_{b} , of the bursts listed in Table 4, give total energies radiated during the bursts $E_{\text{b}} = 4\pi d^2 f_{\text{b}} \approx 1.2 - 7.4 \times 10^{39}$ erg. We can thereby estimate the ignition column of each burst, y_{ign} , through the relation $y_{\text{ign}} = E_{\text{b}}(1+z)/(4\pi R^2 \epsilon_{\text{nuc}})$, where ϵ_{nuc} is the nuclear energy released per unit mass and which can be related to the nuclear energy released per nucleon, $Q_{\text{nuc}} \approx 1.6 + 4X$ MeV nucleon $^{-1}$, by $\epsilon_{\text{nuc}} = Q_{\text{nuc}} \times 10^{18}$ erg g $^{-1}$ (Wallace & Woosley 1981; Fujimoto et al. 1987). This yields ignition columns $y_{\text{ign}} \approx 0.8 - 4.8 \times 10^8$ g cm $^{-2}$.

In turn, theoretical recurrence times for the bursts, $\tau_{\text{rec}} = (y_{\text{ign}}/\dot{m})(1+z)$, can be worked out to be $\approx 0.2 - 43.9 \times 10^5$ s = 0.2 - 5.1 days. We stress that this derivation of τ_{rec} is independent of the assumed distance d . The observed times, Δt , between bursts (Table 4) and these expected recurrence times for pure He combustion, τ_{rec} , match well for bursts 3 and 4 and therefore suggest they were consecutive. The same conclusion holds for bursts 1 and 2, presuming that the persistent flux in between was close to 0.3×10^{-9} erg s $^{-1}$ cm $^{-2}$ though we could not detect it. In order to put stronger constraints on the recurrence time, let us consider the longest uninterrupted data set, i.e. the three consecutive *XMM-Newton* revolutions of April 2007. As the theoretical recurrence time turns out to be nearly twice the measured Δt between bursts 14 and 15, we certainly missed one burst during the data gap in the light curve shown on Fig. 5. In contrast, repeating the previous calculations with a higher hydrogen abundance in the nuclear burning, $X = 0.7$, return shorter recurrence times. In particular for the *XMM-Newton* bursts, τ_{rec} drops to 0.3 day, which means that there should have been two bursts surrounding

Table 4. Bursts parameters.

Id. ^a	Burst Start Time [UTC]	kT_{peak}^b [keV]	R_{peak}^c [km]	$\chi^2/\text{d.o.f.}$	F_{peak}^d	f_b^e	τ_{fit}^f [s]	τ_{calc}^g [s]	F_{pers}^h	Δt^i [s]	γ^j [10^{-3}]
1 JEM-X	2005 Mar 24, 14:26:23	$2.3^{+0.8}_{-0.2}$	7^{+5}_{-3}	15.7/12	$3.2^{+0.7}_{-0.6}$	3.6 ± 0.4	12^{+2}_{-2}	11 ± 3	< 0.3	< 9
2 JEM-X	2005 Mar 25, 22:21:43	$2.0^{+0.2}_{-0.4}$	8^{+3}_{-3}	8.7/9	$2.8^{+0.2}_{-0.6}$	2.6 ± 0.3	8^{+2}_{-1}	9 ± 2	< 0.3	114869	< 11
3 JEM-X	2005 Apr 11, 08:53:16	$1.9^{+0.7}_{-0.5}$	12^{+12}_{-12}	13.7/17	$4.2^{+1.1}_{-3.4}$	4.5 ± 0.5	8^{+2}_{-1}	11 ± 3	0.7 ± 0.2	1420269	17 ± 7
4 JEM-X*	2005 Apr 17, 06:18:54	$2.5^{+0.5}_{-0.4}$	8^{+3}_{-3}	18.4/22	$5.5^{+0.7}_{-1.1}$	12.6 ± 1.0	11^{+2}_{-2}	23 ± 3	0.4 ± 0.2	509114	7.7 ± 4
5 BAT	2007 Jan 22, 06:12:54	$2.4^{+0.4}_{-0.5}$	8^{+3}_{-4}	5.2/7	$5.8^{+1.1}_{-2.5}$	> 4.7	> 8
6 XRT	2007 Feb 16, 22:59:28	$2.7^{+0.8}_{-0.8}$	3.3 ± 0.6	13^{+6}_{-5}	12 ± 6	0.8 ± 0.1	2220459	29 ± 12
7 JEM-X	2007 Mar 02, 08:42:34	$1.6^{+0.3}_{-0.3}$	15^{+8}_{-5}	9.1/13	$3.3^{+0.4}_{-0.5}$	5.3 ± 0.5	16^{+2}_{-3}	16 ± 3	0.7 ± 0.2	1158185	20 ± 6
8 JEM-X	2007 Mar 03, 15:51:05	$1.9^{+0.3}_{-0.3}$	11^{+4}_{-3}	11.6/12	$3.5^{+0.5}_{-1.2}$	3.9 ± 0.4	11^{+1}_{-2}	11 ± 2	1.0 ± 0.2	112057	29 ± 7
9 JEM-X	2007 Mar 06, 22:35:16	$1.6^{+0.4}_{-0.3}$	16^{+13}_{-7}	9.1/11	$3.6^{+0.6}_{-2.3}$	4.3 ± 0.5	10^{+3}_{-2}	12 ± 2	1.3 ± 0.2	283423	36 ± 8
10 JEM-X	2007 Mar 09, 17:28:56	$2.8^{+3.1}_{-1.0}$	4^{+6}_{-4}	5.9/9	$2.8^{+1.2}_{-0.8}$	2.5 ± 0.5	12^{+4}_{-2}	9 ± 4	1.2 ± 0.2	240790	43 ± 20
11 JEM-X	2007 Mar 15, 16:01:05	$1.7^{+0.5}_{-0.4}$	14^{+12}_{-14}	8.1/10	$3.1^{+0.8}_{-2.3}$	2.5 ± 0.4	11^{+2}_{-2}	8 ± 3	1.8 ± 0.2	513094	58 ± 16
12 JEM-X	2007 Mar 16, 14:09:14	$2.2^{+1.0}_{-0.6}$	7^{+6}_{-7}	5.3/8	$2.2^{+0.6}_{-1.9}$	2.0 ± 0.3	12^{+4}_{-3}	9 ± 3	1.4 ± 0.2	79685	65 ± 20
13 JEM-X	2007 Mar 19, 01:15:03	$1.7^{+0.3}_{-0.3}$	15^{+8}_{-5}	3.6/13	$3.9^{+0.7}_{-0.6}$	3.6 ± 0.4	10^{+3}_{-2}	11 ± 2	1.4 ± 0.2	212715	35 ± 8
14 XMM	2007 Mar 31, 01:15:15	$1.9^{+0.6}_{-0.4}$	7^{+3}_{-2}	8.5/9	$1.1^{+0.2}_{-0.6}$	2.5 ± 0.3	19^{+3}_{-2}	21 ± 5	0.6 ± 0.1	1036812	54 ± 17
15 XMM	2007 Apr 02, 02:39:03	$2.2^{+0.4}_{-0.3}$	6^{+2}_{-2}	25.5/21	$1.3^{+0.2}_{-0.3}$	3.6 ± 0.4	21^{+2}_{-2}	28 ± 5	0.7 ± 0.1	177828	54 ± 10

^a Number of the burst, and instrument which detected it. * designates the burst that was also detected by ISGRI.

^b Black-body temperature at the peak of the burst, assuming $N_{\text{H}} = 12 \times 10^{22} \text{ cm}^{-2}$.

^c Black-body radius at the peak assuming a distance of 7 kpc to the source.

^d Unabsorbed bolometric flux (0.1–100 keV) at the peak in units of $10^{-8} \text{ erg s}^{-1} \text{ cm}^{-2}$.

^e Fluence of the burst in units of $10^{-7} \text{ erg cm}^{-2}$.

^f E-folding decay time fitted on the light curve.

^g E-folding decay time calculated with $\tau_{\text{calc}} \equiv f_b/F_{\text{peak}}$.

^h Unabsorbed bolometric persistent flux (0.1–100 keV) prior to the burst in units of $10^{-9} \text{ erg s}^{-1} \text{ cm}^{-2}$.

ⁱ Time elapsed since last detected burst.

^j Ratio of persistent flux to burst flux: $\gamma \equiv F_{\text{pers}}/F_{\text{peak}}$.

burst #15 in the light curve of revolution 1339 on Fig. 5. Since we did not observe such bursts, we conclude that GRS 1741.9–2853 displays pure He bursts.

Now, theoretical works predict the nature of the nuclear burning of the accreted material (H and/or He) during a type-I burst depends critically on the accretion rate of the neutron star (Fujimoto et al. 1981; Bildsten 1998; Peng et al. 2007; Cooper & Narayan 2007). In short, if $0 \lesssim \dot{m}/\dot{m}_{\text{Edd}} \lesssim 0.01$ (i), H burns unstably via the cold CNO cycle and so ignites a mixed He/H explosion. As the fusion of H involves slow β -decays, the rise time and total duration of the burst should be relatively long: ~ 10 s and ~ 100 s, respectively. For $0.01 \lesssim \dot{m}/\dot{m}_{\text{Edd}} \lesssim 0.1$ (ii), H is burned into He steadily through the hot CNO cycle, and a pure He layer develops underneath the surface, which may ignite via the unstable 3α process, thereby producing a pure He burst. The strong interaction at work implies a shorter rise time and total duration (~ 1 s and ~ 10 s, respectively). Finally, if $0.1 \lesssim \dot{m}/\dot{m}_{\text{Edd}} \lesssim 1$ (iii), H is not burned stably fast enough so that a pure He flash triggers a mixed He/H burst with short rise time (~ 1 s) and long duration (~ 100 s). Here, the persistent luminosity of GRS 1741.9–2853 was at the boundary of the two first cases, but as we argued above, the energetics of the bursts suggest a pure He explosion, i.e. case (ii), which is strengthened by the fact that the observed rise times and total durations were short.

As a consistency check, let us discuss the hydrogen depletion condition. Presuming that H burns stably on the surface of the neutron star, i.e. case (ii) or (iii), at a rate fixed by β -decays $\epsilon_{\text{H}} = 5.8 \times 10^{15} \times Z_{\text{CNO}} \text{ erg s}^{-1} \text{ g}^{-1}$ (Hoyle & Fowler 1965) with Z_{CNO} the CNO mass fraction, there is a critical column depth, y_{d} , above which H is completely depleted leaving only He for the explosion. y_{d} thus fixes the boundary between cases (ii) and (iii). In the steady-state, H burns stably as fast

as it is accreted, giving $y_{\text{d}} = X_0 \dot{m} E_{\text{H}} / \epsilon_{\text{H}}$ (Cumming & Bildsten 2000) where $E_{\text{H}} \approx 6.0 \times 10^{18} \text{ erg g}^{-1}$ is the energy release in the hot CNO cycle including neutrino energy losses (Wallace & Woosley 1981). Let us consider the most intense burst, #4, which has $y_{\text{ign}} \approx 4.8 \times 10^8 \text{ g cm}^{-2}$. Even in the most extreme case of pure H accretion ($X_0 = 1$), we always find $y_{\text{ign}} > y_{\text{d}}$ as long as $Z_{\text{CNO}} > 0.004$. Since a CNO abundance of 0.004 for the companion star is relatively low for a population II low-mass star, we are confident that this condition on the metallicity is fulfilled and thereby that burst 4 was a pure He burst (case (ii)). The conclusion of the comparison between the depletion and ignition columns is not as straightforward for the other bursts though, as the assumed values for X_0 and Z_{CNO} turn out to be more critical. We note however that GRS 1741.9–2853 possibly lies in the central molecular zone of the GC, where Najarro et al. (2009) recently measured the CNO composition to be up to twice solar, $Z_{\text{CNO}} = 0.02$ (see Asplund et al. 2005, for solar abundances). Besides, provided the donor star is an evolved low-mass star with a He-rich composition ($X_0 < 0.3$), we again find $y_{\text{ign}} > y_{\text{d}}$ for all the bursts. But in view of the high uncertainties on the true values of X_0 and Z_{CNO} , we stress that this depletion condition which consolidates case (ii) should only be regarded as suggestive.

Kuulkers et al. (2008) recently raised the issue of bursts during the quiescent state of a soft X-ray transient (SXT) and the possible role of trigger they may play for the SXT outburst itself. For GRS 1741.9–2853, the burst seen by *Swift*/BAT in January 2007 would be a good candidate for a trigger of the 2007 outburst. But the detection of a short activity period, prior to the long 2007 one, in September 2006 (Degenaar & Wijnands 2009) points to the fact that the companion star was already dumping a substantial amount of matter towards the neutron star at the time. In all likelihood, this helped the SXT outburst develop and then paved the way for type-I bursts, and not the opposite. On top of

that, it is very implausible that the source produces bursts during its quiescent state at 10^{32-33} erg s⁻¹. This is theoretically motivated by the expected stability of hydrogen burning via the *pp*-process or pycnonuclear reactions below 10^{33} erg s⁻¹ (Fushiki & Lamb 1987). This is also observationally corroborated by the non-detection of type-I bursts at this luminosity level up to now (Table 1). Note that we explored 2.8 Ms of quiescent state with *INTEGRAL* over four years without success. Moreover, at 10^{33} erg s⁻¹, it would already take five years to accumulate the necessary fuel on the neutron star surface for a burst with a characteristic energy release $\sim 10^{39}$ erg. So it looks as though GRS 1741.9–2853 gives rise to thermonuclear explosions only when accreting at a luminosity level in excess of 10^{35-36} erg s⁻¹.

While "burst-only sources" have often been put forward as prototypes for the poorly observed H burning bursts at low accretion rates, i.e. case (i), and potentially during quiescence, it seems from this discussion that GRS 1741.9–2853 is a member of the faint transient class exhibiting pure helium runaways, i.e. case (ii), only when in outburst. This is another indication that the "burst-only sources" should maybe not be held as a distinctive class. Cornelisse et al. (2004), indeed, already alluded to the fact that the burst-only sources do not form a separate homogeneous group, based on the discrepancies in the bursts durations and the nature of the system (faint transient or quiescent neutron star transients).

5. Conclusions

Since its discovery, GRS 1741.9–2853 has not been an easy target for X-ray missions, because it is transient, faint and located in a region affected by source confusion. As a consequence, the detailed analysis of its bursting behavior needs long exposures, high resolution and sensitivity, which could finally be achieved with *INTEGRAL*, *XMM-Newton*, and *Swift*. In this paper we essentially analyzed all the data on GRS 1741.9–2853 ever recorded by the two first satellites since 2002. We confirm what had been found by other instruments earlier, i.e. that the source is at a distance of ~ 7 kpc and exhibits bursts only when in outburst, every couple of years. From the discovery of 15 new bursts in 2005/2007 and the spectral fitting of the contemporaneous persistent emission, we were able to investigate the nuclear burning processes powering the explosions. We find that unstable pure He fusion matches well the observations, whereas the presence of H would contradict the measured recurrence times and bursts durations. In addition, bursts oscillations have been proposed to be present in some bursts of GRS 1741.9–2853 by Galloway et al. (2008), which is in line with the fact that these oscillations appears mostly in helium burning runaways (Cumming & Bildsten 2000; Narayan & Cooper 2007). However, the existence of a fast spinning neutron star in GRS 1741.9–2853 is still something that future work with current X-ray facilities need to conclusively demonstrate.

Acknowledgements. GT wishes to warmly thank M. Renaud, J. Chenevez, D. Götz, F. Mattana, G. Ponti, and J.A. Zurita Heras for valuable discussions and help regarding several aspects of the *INTEGRAL* and *XMM-Newton* data analysis. EB is grateful to M. Perri for his help with the *Swift* data analysis. MF acknowledges the French Space Agency (CNES) for financial support. Part of this work has been funded by the french Agence Nationale pour la Recherche (ANR) through grant ANR-06-JC-0047.

INTEGRAL is an ESA project with instruments and science data center funded by ESA member states (especially the PI countries: Denmark, France, Germany, Italy, Switzerland, and Spain), the Czech Republic, and Poland, and with the participation of Russia and the US. The *XMM-Newton* project is an ESA Science Mission with instruments and contributions directly funded by ESA Member States and the USA (NASA).

References

- Arnaud, K. A. 1996, in *Astronomical Society of the Pacific Conference Series*, Vol. 101, *Astronomical Data Analysis Software and Systems V*, ed. G. H. Jacoby & J. Barnes
- Asplund, M., Grevesse, N., & Sauval, A. J. 2005, in *Astronomical Society of the Pacific Conference Series*, Vol. 336, *Cosmic Abundances as Records of Stellar Evolution and Nucleosynthesis*, ed. T. G. Barnes, III & F. N. Bash, 25
- Bildsten, L. 1998, in *NATO ASIC Proc. 515: The Many Faces of Neutron Stars*, ed. R. Buccheri, J. van Paradijs, & A. Alpar, 419
- Brandt, S., Budtz-Jørgensen, C., Lund, N., et al. 2003, *A&A*, 411, L243
- Chelovekov, I. V., Grebenev, S. A., & Sunyaev, R. A. 2007, *ArXiv:0709.2328*
- Cocchi, M., Bazzano, A., Natalucci, L., et al. 2001, *A&A*, 378, L37
- Cocchi, M., Bazzano, A., Natalucci, L., et al. 1999, *A&A*, 346, L45
- Cooper, R. L. & Narayan, R. 2007, *ApJ*, 661, 468
- Cornelisse, R., in 't Zand, J. J. M., Kuulkers, E., et al. 2004, *Nuclear Physics B Proceedings Supplements*, 132, 518
- Cornelisse, R., in 't Zand, J. J. M., Verbunt, F., et al. 2003, *A&A*, 405, 1033
- Courvoisier, T. J.-L., Walter, R., Beckmann, V., et al. 2003, *A&A*, 411, L53
- Cumming, A. & Bildsten, L. 2000, *ApJ*, 544, 453
- Degenaar, N. & Wijnands, R. 2009, *A&A*, 495, 547
- Dodds-Eden, K., Porquet, D., Trap, G., et al. 2009, *ArXiv:0903.3416*
- Falanga, M. 2008, in *American Institute of Physics Conference Series*, Vol. 1054, 157–171
- Falanga, M., Chenevez, J., Cumming, A., et al. 2008, *A&A*, 484, 43
- Falanga, M., Cumming, A., Bozzo, E., & Chenevez, J. 2009, *A&A*, 496, 333
- Fox, D. B., Barthelmy, S. D., & Markwardt, C. B. 2007, *GCN Circular*, 6020
- Fujimoto, M. Y., Hanawa, T., & Miyaji, S. 1981, *ApJ*, 247, 267
- Fujimoto, M. Y., Sztajno, M., Lewin, W. H. G., & van Paradijs, J. 1987, *ApJ*, 319, 902
- Fushiki, I. & Lamb, D. Q. 1987, *ApJ*, 323, L55
- Galloway, D. K., Muno, M. P., Hartman, J. M., Psaltis, D., & Chakrabarty, D. 2008, *ApJS*, 179, 360
- Gehrels, N., Chincarini, G., Giommi, P., et al. 2004, *ApJ*, 611, 1005
- Goldwurm, A. 1996, *Memorie della Societa Astronomica Italiana*, 67, 121
- Goldwurm, A., David, P., Foschini, L., et al. 2003, *A&A*, 411, L223
- Heise, J., in 't Zand, J. J. M., Smith, M. J. S., et al. 1999, *Astrophysical Letters Communications*, 38, 297
- Hoyle, R. & Fowler, W. A. 1965, in *Quasi-Stellar Sources and Gravitational Collapse*, ed. I. Robinson, A. Schild, & E. L. Shucking (Chicago Univ. Press), 17
- in 't Zand, J. 2001, in *ESA Special Publication*, Vol. 459, *Exploring the Gamma-Ray Universe*, ed. A. Gimenez, V. Reglero, & C. Winkler, 463–470
- Jansen, F., Lumb, D., Altieri, B., et al. 2001, *A&A*, 365, L1
- King, A. R. 2000, *MNRAS*, 315, L33
- King, A. R. & Ritter, H. 1998, *MNRAS*, 293, L42
- Kuulkers, E., den Hartog, P. R., in 't Zand, J. J. M., et al. 2003, *A&A*, 399, 663
- Kuulkers, E., in 't Zand, J. J. M., & Lasota, J. P. 2008, *ArXiv:0809.3323*
- Kuulkers, E., Shaw, S., Chenevez, J., et al. 2007a, *The Astronomer's Telegram*, 1005, 1
- Kuulkers, E., Shaw, S., Chenevez, J., et al. 2007b, *The Astronomer's Telegram*, 1008, 1
- Kuulkers, E., Shaw, S. E., Paizis, A., et al. 2007c, *A&A*, 466, 595
- Lasota, J.-P. 2001, *New Astronomy Review*, 45, 449
- Laycock, S., Zhao, P., Torres, M. A. P., et al. 2005, *The Astronomer's Telegram*, 522, 1
- Lebrun, F., Leray, J. P., Lavocat, P., et al. 2003, *A&A*, 411, L141
- Lewin, W. H. G., van Paradijs, J., & Taam, R. E. 1993, *Space Science Reviews*, 62, 223
- Liu, Q. Z., van Paradijs, J., & van den Heuvel, E. P. J. 2007, *A&A*, 469, 807
- Lund, N., Budtz-Jørgensen, C., Westergaard, N. J., et al. 2003, *A&A*, 411, L231
- Mereghetti, S., Götz, D., Borkowski, J., Walter, R., & Pedersen, H. 2003, *A&A*, 411, L291
- Muno, M., Baganoff, F., & Arabadjis, J. 2003, *ApJ*, 598, 474
- Muno, M. P., Bauer, F. E., Bandyopadhyay, R. M., & Wang, Q. D. 2006, *ApJS*, 165, 173
- Muno, M. P., Wijnands, R., Wang, Q. D., et al. 2007, *The Astronomer's Telegram*, 1013, 1
- Najarro, F., Figuer, D. F., Hillier, D. J., Geballe, T. R., & Kudritzki, R. P. 2009, *ApJ*, 691, 1816
- Narayan, R. & Cooper, R. L. 2007, *ApJ*, 665, 628
- Peng, F., Brown, E. F., & Truran, J. W. 2007, *ApJ*, 654, 1022
- Porquet, D., Grosso, N., Goldwurm, A., et al. 2007, *The Astronomer's Telegram*, 1058, 1
- Porquet, D., Grosso, N., Predehl, P., et al. 2008, *A&A*, 488, 549
- Sakano, M., Koyama, K., Murakami, H., Maeda, Y., & Yamauchi, S. 2002, *ApJS*, 138, 19
- Strohmayer, T. & Bildsten, L. 2006, *New views of thermonuclear bursts*

- (Compact stellar X-ray sources), 113–156
- Strohmayer, T. E., Jahoda, K., Giles, A. B., & Lee, U. 1997, *ApJ*, 486, 355
- Sunyaev, R. 1990, *IAU Circ.*, 5104, 1
- Sunyaev, R., Pavlinskii, M., Churazov, M. G. E., et al. 1991, *Astronomy Letters*, 17, 42
- Trap, G., Goldwurm, A., Terrier, R., et al. 2009, in *Proceedings of the 7th INTEGRAL Workshop, An INTEGRAL View of Compact Objects*, PoS(Integral108)047
- Ubertini, P., Lebrun, F., Di Cocco, G., et al. 2003, *A&A*, 411, L131
- Wallace, R. K. & Woosley, S. E. 1981, *ApJS*, 45, 389
- Westergaard, N. J., Kretschmar, P., Oxborrow, C. A., et al. 2003, *A&A*, 411, L257
- Wijnands, R. 2006, in *Bulletin of the American Astronomical Society*, Vol. 38, 1183
- Wijnands, R. 2008, *Proceedings of "A decade of accreting millisecond pulsars"*
- Wijnands, R., in't Zand, J. J. M., Rupen, M., et al. 2006, *A&A*, 449, 1117
- Wijnands, R., Klien Wolt, M., Kuulkers, E., et al. 2007, *The Astronomer's Telegram*, 1006, 1
- Wijnands, R., Maccarone, T., Miller-Jones, J., et al. 2005, *The Astronomer's Telegram*, 512, 1
- Winkler, C., Courvoisier, T. J.-L., Di Cocco, G., et al. 2003, *A&A*, 411, L1